# The Orientation of Nisin in Membranes

Breukink, Eefjan; Kraaij, Cindy van; Dalen, Annemieke van; Demel, Rudy A.; Siezen, Roland J.; Kruijff, Ben de; Kuipers, Oscar

Link to publication in University of Groningen/UMCG research database

# The Orientation of Nisin in Membranes[†]

Eefjan Breukink,*,[‡] Cindy van Kraaij,[‡,§] Annemieke van Dalen,[‡] Rudy A. Demel,[‡] Roland J. Siezen,[§] Ben de Kruijff,[‡] and Oscar P. Kuipers[§]

*Department Biochemistry of Membranes, Centre for Biomembranes and Lipid Enzymology, Institute of Biomembranes, Utrecht University, Padualaan 8, 3584 CH, Utrecht, The Netherlands, and Microbial Ingredients Section, Netherlands Institute of Dairy Research (NIZO), P.O. Box 20, 6710 BA, Ede, The Netherlands*

ABSTRACT: Nisin is a 34 residue long peptide belonging to the group A lantibiotics with antimicrobial activity against Gram-positive bacteria. The antimicrobial activity is based on pore formation in the cytoplasmic membrane of target organisms. The mechanism which leads to pore formation remains to be clarified. We studied the orientation of nisin via site-directed tryptophan fluorescence spectroscopy. Therefore, we engineered three nisin Z variants with unique tryptophan residues at positions 1, 17, and 32, respectively. The activity of the tryptophan mutants against Gram-positive bacteria and in model membrane systems composed of DOPC or DOPG was established to be similar to that of wild type nisin Z. The tryptophan fluorescence emission maximum showed an increasing blue-shift upon interaction with vesicles containing increased amounts of DOPG, with the largest effect for the 1W peptide. Studies with the aqueous quencher acrylamide showed that all tryptophans became inaccessible from the aqueous phase in the presence of negatively charged lipids in the vesicles. From these results it is concluded that anionic lipids mediate insertion of the tryptophan residues in at least three positions of the molecule into the lipid bilayer. The depth of insertion of the tryptophan residues was determined via quenching of the tryptophan fluorescence by spin-labeled lipids. The results showed that the depth of insertion was dependent on the amount of negatively charged lipids. In membranes containing 50% DOPG, the distances from the bilayer center were determined to be 15.7, 15.0, and 18.4 Å for the tryptophan at position 1, 17, and 32, respectively. In membranes containing 90% DOPG, these distances were calculated to be 10.8, 11.5, and 13.1 Å, respectively. These results suggest an overall parallel average orientation of nisin in the membrane, with respect to the membrane surface, with the N-terminus more deeply inserted than the C-terminus. These data were used to model the orientation of nisin in the membrane.

Nisin has antimicrobial activity against a broad spectrum of Gram-positive bacteria and is widely used in the food industry as a safe and natural preservative (*1*). It is a positively charged amphiphilic peptide of 34 amino acids of which 13 are post-translationally modified (Figure 1). These modifications include the dehydration of serine and threonine, resulting in three dehydroalanine and five dehydrobutyrine residues. Five of these dehydro residues are subsequently linked to the sulfhydryl groups of the five cysteine residues present in pre-nisin Z, resulting in the thioether bond of the characteristic (β-methyl)lanthionine rings (*2, 3*). The nisin activity against growing cells is primarily thought to arise from pore formation in the cytoplasmic membrane of the target organism.

Model membrane systems have been used extensively to study the lipid dependency of the nisin-membrane interaction (*4−8*). Recently, several research groups have shown that

the activity of nisin in vitro is largely dependent on the presence of negatively charged lipids for both model (*9−11*) and bacterial membrane systems (*9*). The binding of nisin to the membrane was shown to be primarily mediated by the C-terminal region (*9*). Nisin binding is followed by penetration into the lipid phase of the membrane since nisin was shown to be able to insert into monolayers in an anionic lipid-dependent way (*9, 12*).

The topology of nisin in the membrane is unknown, but is an important aspect of the mode of action of nisin. To determine this topology, we used tryptophan fluorescence spectroscopy which is a powerful tool to study the membrane association of peptides. Since nisin does not naturally contain tryptophan residues, we used site-directed tryptophan fluorescence with nisin variants with unique tryptophan residues at positions 1, 17, and 32. Analysis of emission spectra and fluorescence quenching by water-soluble agents was used to characterize the peptide−membrane association. Depth-dependent quenching of fluorescence by spin-labeled lipids has been proven to be a valuable tool to determine the topology of tryptophan- or tyrosine-containing peptides in membranes (*13−16*) and was used to determine the depth of penetration. Quenching depends on the distance between the tryptophan residue and the spin-label and occurs over a very short distance (*17*), rendering this method very useful

* Corresponding author: Tel: +31 30 2533342. Fax: +31 30 2522478. E-mail: e.j.breukink@chem.ruu.nl.
[‡] Utrecht University.
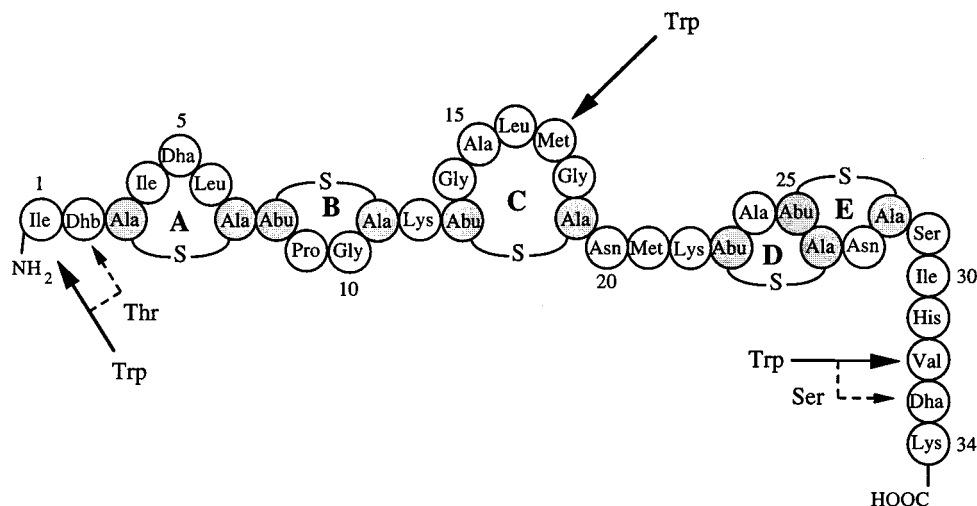[§] Netherlands Institute of Dairy Research.

FIGURE 1: Primary structure of nisin Z. The nisin Z single tryptophan variants used in this study are indicated by arrows. The dotted arrows indicate lack of modification at residue 2 and 33. Dha = dehydroalanine, Dhb = dehydrobutyrine, Ala-S-Ala = lanthionine, Abu-S-Ala = $\beta$-methyllanthionine.

to determine penetration depth. The results showed that nisin has an overall parallel orientation with respect to the membrane surface, with the N-terminus deeper inserted in the membrane than the C-terminus.

## MATERIALS AND METHODS

*Materials.* Nisin Z was produced and purified as described (*18*). The tryptophan-nisin Z mutants I1W, M17W (*12, 19*), and V32W (*20*) were obtained by site-directed mutagenesis and analyzed as described (*20*). Nisin stock solutions were stored at $-80$ °C in 0.05% acetic acid. Protein concentrations were determined using the bicinchoninic acid protein assay reagent with bovine serum albumin as a standard (Pierce Chemical Corporation). 1,2-Dioleoyl-*sn*-glycero-3-phosphocholine (DOPC),[1] 1,2-dioleoyl-*sn*-glycero-3-phosphoglycerol (DOPG), 1,2-dioleoyl-*sn*-glycero-3-phosphoethanolamine (DOPE), 1,2-dioleoyl-*sn*-glycero-3-phosphotempocholine (0-SLPC), 1-palmitoyl-2-(5-doxyl)-stearoyl-*sn*-glycero-3-phosphocholine (5-SLPC), and 1-palmitoyl-2-(12-doxyl)-stearoyl-*sn*-glycero-3-phosphocholine (12-SLPC) were purchased from Avanti Polar Lipids Inc. Carboxyfluorescein was purchased from Kodak and purified as described (*21*). All other chemicals were of analytical grade or better.

*Purification and Characterization of Nisin Mutants.* The purification of the mutant nisin peptides was performed as described (*18*), and the purity of the mutant nisins was confirmed by analytical RP-HPLC (*20*). Introduction of a tryptophan residue at position 1 resulted in partial inhibition of dehydration of threonine at position 2. Thus, from the

supernatant of an I1W producing strain, two products were purified, I1W and I1W/Dhb2T. The latter nisin Z variant was used in the tryptophan fluorescence experiments. It was furthermore shown (*20*) that substitution of Val-32 by Trp resulted in an unmodified serine at position 33. This second mutation does not affect the activity of nisin Z (*20*). For reasons of clarity, the mutants are called 1W, 17W, and 32W.

*Minimal Inhibitory Concentration (MIC) Determination.* The minimal inhibitory concentration was determined by measuring the inhibition of growth of the indicator strains *Micrococcus flavus* and *Streptococcus thermophilus* in a liquid bioassay as described (*18*).

*Vesicle Preparation.* Large unilamellar vesicles were formed by the extrusion technique (*22*), according to the protocol described previously (*9*). Phospholipid concentration was determined as inorganic phosphate after destruction of the phospholipids by perchloric acid (*23*).

*Monolayer and Leakage Experiments.* Monolayer, potassium, and carboxyfluorescein leakage experiments were performed as described (*9*).

*Tryptophan Fluorescence Measurements.* All fluorescence measurements were performed in 1.25 mL of 50 mM Mes, 100 mM $K_2SO_4$, pH 6.0, using an SLM-Aminco SPF-500 C fluorimeter. The solution in the cuvette was kept at 20 °C and continuously stirred. The tryptophan residue of the nisin mutants was excited at 280 nm (bandwidth 5 nm) and the emission was read either at 340 or at 350 nm (bandwidth 10 nm) as indicated. The fluorescence data were corrected (1) for the vesicle blank (scatter) which at the maximal lipid concentration used contributed at most 25% to the total signal, (2) for dilution effects, and (3) for the inner-filter effect. The latter correction factor was determined in a parallel experiment using equal amounts of the free amino acid tryptophan (*24*), which showed no interaction with the lipid systems tested, and wild type nisin Z. This correction factor contributed at most 5−10% to the signal.

*Emission Spectra and Intensity Measurements.* Emission spectra were recorded with 1.0 $\mu$M mutant peptide from 300 to 400 nm (bandwidth 5 nm) in the absence or presence of vesicles of the indicated composition at a concentration of 100 $\mu$M lipid-Pi. The dependency of the fluorescence

intensity on the negatively charged lipid content of the vesicles was determined by varying the DOPC/DOPG ratio.

*Binding Experiments.* Binding of nisin to phospholipid vesicles was studied by following the changes in fluorescence intensity at an emission wavelength (350 nm for M17W and V32W; 340 nm for I1W) upon addition of vesicles. For this purpose, small aliquots of a concentrated vesicle solution (~15 mM lipid-Pi) were added, up to a maximum of 150 $\mu$M lipid-Pi, to solutions of 1.0 $\mu$M nisin mutant in buffer, and after stabilization of the signal, the fluorescence intensity was determined. Each point in this titration was measured using independent samples. The relative fluorescence intensity ($F/F_0$, with $F$ and $F_0$ the corrected fluorescence intensity in the presence and absence of lipid, respectively) was plotted against the lipid concentration. These titration curves were quantitatively analyzed according to the following relationship:

$$\epsilon - 1 = (\epsilon_b - 1) - K_d(\epsilon - 1)/mn \quad (1)$$

$K_d$ is the dissociation constant of the lipid−peptide complex, $m$ denotes the lipid concentration, and $n$ is the number of binding sites per lipid. $\epsilon$ represents $F/F_0$, the relative change of the fluorescence intensity, and $\epsilon_b$ the maximum relative change of the fluorescence intensity attainable when all peptide is bound. The parameter $K_d/n$, which is obtained as the slope of a plot of $\epsilon - 1$ vs ($\epsilon - 1$)/$m$, provides a reliable criterion for comparing the lipid affinities of the various peptides (*25*). This approach for analysis of the titration curves is an empirical one, which does not account for the effect of electrostatic interactions on the surface concentration of the peptides, but was chosen to enable us to compare our data with earlier published results of another nisin tryptophan variant (*11*).

*Acrylamide Quenching Experiments.* Acrylamide quenching experiments were carried out at an excitation wavelength of 295 nm to reduce the absorbance by acrylamide (*26*). Small aliquots of acrylamide were added from a 3.0 M stock solution to 1.0 $\mu$M nisin mutant in the absence or in the presence of DOPG, DOPG/DOPC (1:1) or DOPC vesicles (150 $\mu$M lipid-Pi).

The data were analyzed according to the Stern−Volmer equation (*27*):

$$F_0/F = 1 + K_{SV}[Q] \quad (2)$$

where $F_0$ and $F$ are the fluorescence intensities in the absence and the presence of quencher (Q), respectively. $K_{SV}$ is the Stern−Volmer quenching constant, which is a measure for the accessibility of the tryptophan to acrylamide, provided that there are no differences in fluorescence lifetime. This $K_{SV}$ was calculated as the slope of the Stern−Volmer plot, which is linear for acrylamide concentrations up to 60 mM (*26*).

*Spin-Labeled Lipid Quenching Experiments.* To examine the depth of the tryptophan residue of the different nisin mutants in the membrane bilayer, vesicles were prepared containing 10 mol % spin-labeled PC. The spin content of the vesicles was not checked, which could lead to an error in the absolute (but not relative) depth value. The change of fluorescence intensity upon addition of 100 $\mu$M lipid-Pi of the spin-labeled vesicles to a solution of 1.0 $\mu$M nisin

mutant ($F$) was compared to the fluorescence intensity change upon addition of the same amount of vesicles containing unlabeled PC ($F_0$). The data were analyzed as quenching efficiencies, according to

$$\text{quenching efficiency} = (1 - F/F_0) \times 100\% \quad (3)$$

The differences in quenching of the tryptophan fluorescence depending on the position of the spin-label was used to calculate the most probable location of the fluorophore in the membrane by two methods, i.e., the parallax method developed by Chattopadhyay and London (1987) and the distribution analysis developed by Ladhokin et al. (1993). In the first method, the depth of the tryptophan residue was calculated as

$$Z_{cf} = L_{c1} + [(-\ln(F_1/F_2)/\pi C) - L_{21}^{2}]/2L_{21} \quad (4)$$

where $Z_{cf}$ is the distance of the fluorophore from the center of the bilayer, $L_{c1}$ is the distance of the shallow quencher from the center of the bilayer, $F_1$ is the fluorescence intensity in the presence of the shallow quencher, $F_2$ is the fluorescence intensity in the presence of the deeper quencher, $L_{21}$ is the distance between the shallow and deep quenchers, and $C$ is the concentration of quencher in molecules/$\text{Å}^2$.

In the second method, the depth of the tryptophan residue is calculated by fitting the data to the following equation:

$$\ln[F(h)/F_0] = S/(\sigma\sqrt{2\pi})\exp\{-1/2[(h - h_m)/\sigma]^2\} \quad (5)$$

where $F(h)$ is a set of intensities measured as a function of vertical distance from the bilayer center to the quencher ($h$), $F_0$ is the intensity in the absence of spin-labeled lipids, $S$ is the area under the curve (a measure of the effectiveness of quenching), $\sigma$ is the dispersion (a measure for the distribution of the depth in the bilayer), and $h_m$ is the most probable position of the fluorophore.

In these two methods of calculation, the following values for the depth (distance from the bilayer center) of the spin-labels were used: for 0-SLPC 19.5 Å (*28*), for 5-SLPC and 12-SLPC, and 12.15 and 5.85 Å, respectively (*17*).

*Effect of Membrane Potential.* The effect of a membrane potential on the orientation of nisin was tested with use of DOPG/DOPC (1:1) and (9:1) vesicles containing 10 mol % of one of the above-described spin-labeled PCs. A trans-membrane $K_{in}^{+}/Na_{out}^{+}$ gradient was obtained by diluting the vesicles 130 times in 50 mM Mes-NaOH, pH 6.0, and 100 mM $Na_2SO_4$. A trans-membrane potential (negative inside) was induced by adding valinomycin (1 $\mu$g/mL in ethanol) in a 1:10$^4$ molar ratio with respect to phospholipid. The amount of quenching of the fluorescence of 0.5 $\mu$M tryptophan variant by spin-label containing vesicles (250 $\mu$M lipid-Pi, final concentration) in the presence of a membrane potential was compared to the amount of quenching in the absence of a membrane potential. A different amount of quenching would suggest a different location of the tryptophan in the bilayer, hence a different orientation of nisin in the membrane.

*Modeling.* The family of NMR structures of nisin A in the presence of DPC micelles (*29*) was used to estimate the orientation of nisin in the membrane. The 15 available NMR structures were each converted such that they contained three

Table 1: Characterization of the Nisin Tryptophan Mutants Using Different Assays

| | MIC values ($\mu$g/L) against | | surface pressure increase[a] (mN/m)[d] | | potassium leakage rate[b] (%/s)[d] | CF leakage rate[c] (%/s)[d] |
|---|---|---|---|---|---|---|
| | *M. flavus* | *S. thermophilus* | DOPC | DOPG | | |
| nisin Z | 11 | 6 | $2.3 \pm 0.6$ | $7.1 \pm 0.2$ | $0.30 \pm 0.03$ | $2.8 \pm 0.3$ |
| 1W | 18 | 41 | $2.1 \pm 0.2$ | $6.3 \pm 0.3$ | $0.28 \pm 0.02$ | $1.6 \pm 0.2$ |
| 17W | 22 | 50 | $1.5 \pm 0.2$ | $8.8 \pm 0.2$ | $0.26 \pm 0.02$ | $1.9 \pm 0.2$ |
| 32W | 30 | 20 | $1.6 \pm 0.1$ | $8.4 \pm 0.2$ | $0.34 \pm 0.03$ | $0.6 \pm 0.1$ |

[a] The initial surface pressure was 25 mN/m, the peptide concentration was 0.6 $\mu$M. [b] The lipid concentration was 30 $\mu$M on Pi basis, the peptide concentration was 1.2 $\mu$M. [c] The lipid concentration was 25 $\mu$M on Pi basis, the peptide concentration was 1 $\mu$M. [d] $N = 3$.

tryptophans at positions 1, 17, and 32. This conversion was done with the program O (*30*), which positions the side chain according to the backbone structure with reference to a database consisting of 32 protein structures that have been refined at high resolution.

For each structure, it was tried to visually orient the peptide such that the tryptophans are positioned according to their determined depths with respect to the center of the bilayer. Structures which either could not be oriented in such a way or would place a lysine residue deep in the hydrophobic phase of the bilayer were omitted.

## RESULTS

*Characterization of the Tryptophan Mutants.* To ensure that the nisin tryptophan variants are good representatives of native nisin Z, they were tested for antimicrobial activity and for their activities in model membrane systems, i.e., insertion into monolayers and induction of potassium and carboxyfluorescein leakage from vesicles.

The antimicrobial activities of the tryptophan variants were determined as minimal inhibitory concentration (MIC) values against two indicator strains *Micrococcus flavus* DSM1790 and *Streptococcus thermophilus* Rs. The MIC values of the tryptophan mutants for *M. flavus* are 2–3-fold higher as compared to wild type nisin Z (Table 1). For *S. thermophilus*, a strain more sensitive to nisin Z, the MIC values of the tryptophan containing peptides were 3–8-fold higher as compared to wild type (Table 1). Apparently, the antimicrobial activity of the mutant peptides is somewhat lower as compared to wild type nisin Z. However, these differences in biological activity could, besides from differences in membrane interaction, be caused by other factors such as different interactions with the cell wall. Therefore, we tested the membrane interaction of the mutant peptides also in model systems composed of zwitterionic lipid DOPC or negatively charged DOPG.

Membrane insertion of the tryptophan mutants was analyzed via the monolayer technique. Table 1 shows that all mutant peptides cause similar increases in surface pressure in DOPC and DOPG monolayers as wild type nisin Z and that insertion in the DOPG system is highly favored.

Nisin-induced leakage of solutes from model vesicles has proven to be a valuable tool to study the differences in membrane-interaction of nisin mutants compared to wild type nisin (*9–11*). We tested the tryptophan-containing peptides in both a potassium leakage assay as well as in a carboxyfluorescein (CF) leakage assay. The three mutant peptides induced K$^+$ leakage to a similar extent as wild type nisin Z (Table 1). The activity of 1W and 17W in the CF leakage assay was slightly lower (a factor of 1.5–2) as compared to that of wild type nisin Z (Table 1). 32W showed the lowest
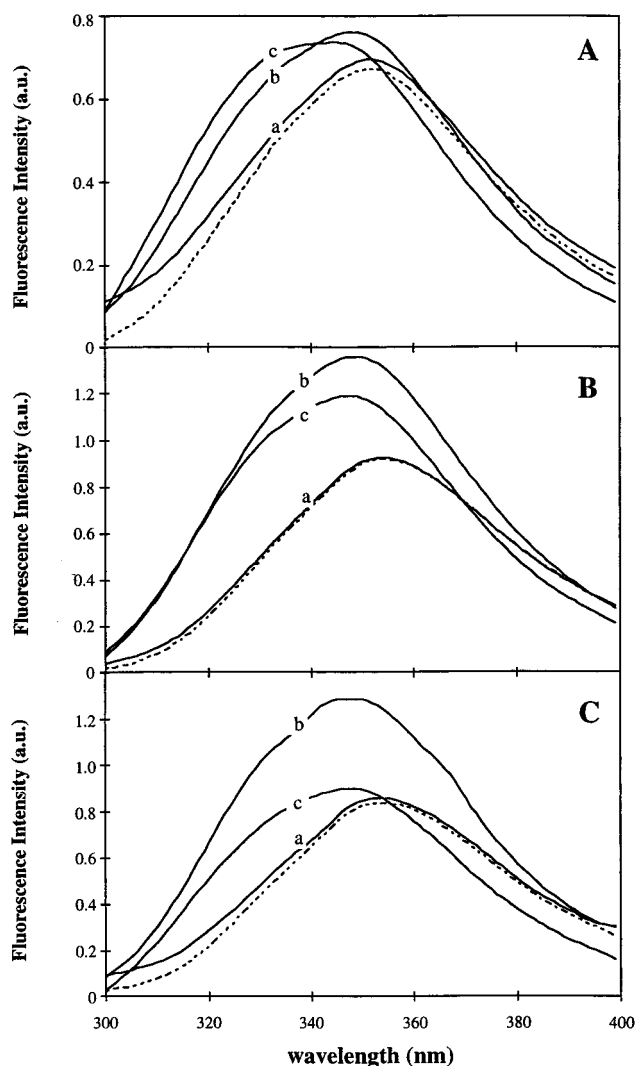


FIGURE 2: Fluorescence emission spectra of 1 $\mu$M nisin tryptophan mutant in the presence of 100 $\mu$M vesicles (lipid-Pi) of DOPC (tracing a), DOPC/DOPG (1:1) (tracing b), DOPG (tracing c) or in the absence of lipids (dotted line). (A) 1W, (B) 17W, (C) 32W.

activity in this assay (approximately 5 times lower). In both assays, anionic lipids stimulate leakage induced by the mutants to a similar extent as wild type nisin Z (not shown). These studies show that the tryptophan mutants are valid representatives of nisin Z.

*Tryptophan Fluorescence. Emission Spectra.* Emission spectra of 1W, 17W, and 32W were recorded in the absence or presence of vesicles of different phospholipid composition (Figure 2). All three peptides in buffer showed maximal fluorescence emission at 352 nm (Figure 2, dotted lines), typical for tryptophan in a polar environment (*25*). Upon addition of DOPC vesicles, hardly any effect was observed

Table 2: Blue-Shifts (nm) of the Emission Maximum of the Nisin Z-Tryptophan Mutants (1 $\mu$M) in the Presence of Vesicles (100 $\mu$M Lipid-Pi) of Different Composition

|      | DOPC | DOPC/DOPG (1:1) | DOPG |
|------|------|-----------------|------|
| 1W   | 0    | 2               | 12   |
| 17W  | 0    | 5               | 7    |
| 32W  | 0    | 5               | 7    |
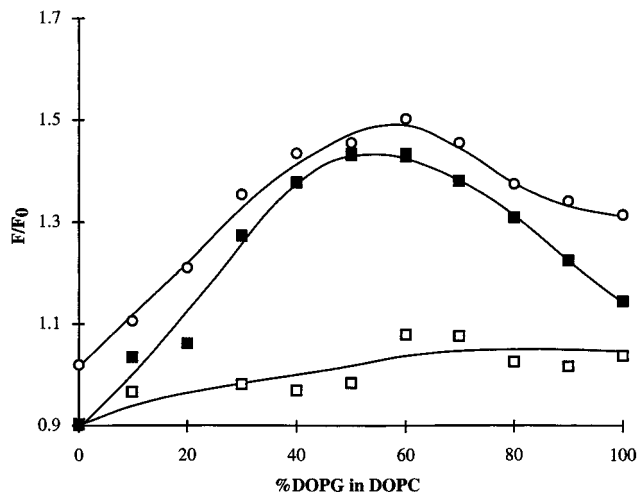


FIGURE 3: Fluorescence intensity of 1 $\mu$M for 1W (□) at 340 nm, 17W (○), and 32W (■) at 350 nm, as a function of the increasing DOPG concentrations.

(Figure 2, tracing a). Only for 1W a small intensity increase could be observed, but no blue-shift (Figure 2A, tracing a). Addition of vesicles containing negatively charged lipids induced changes in the tryptophan spectra of all three peptides. 1W, 17W, and 32W showed an increasing blue-shift of the emission maximum with increasing concentrations of DOPG (Figure 2, tracings b and c), indicating that the tryptophan residues are located in a more apolar environment. This implies that the tryptophan residues at the three positions are inserted into the lipid phase of the membrane. Table 2 summarizes the blue-shifts of the mutant peptides in the presence of vesicles of different composition. 1W showed the largest blue-shift (12 nm) as compared to 17W and 32W (both 7 nm) in the presence of pure PG vesicles, while in the presence of PG/PC (1:1) vesicles, the blue-shift was intermediate. In general, a blue-shift of the fluorescence maximum caused by moving into a more hydrophobic environment is accompanied by a proportional fluorescence intensity increase. Figure 2 showed that this was observed for all peptides in the PG/PC (1:1) system. However, in the presence of pure PG vesicles the peptides showed a disproportional intensity increase relative to the increased blue-shift. Therefore, we examined the anionic lipid dependency of the fluorescence intensity increase in more detail by determining the relative fluorescence intensity in the presence of 100 $\mu$M vesicles (lipid-Pi) containing increasing ratios of DOPG over DOPC. Figure 3 shows that the fluorescence intensity of 1W remains low in the presence of vesicles of different composition. However, 17W and 32W showed the expected increase of the fluorescence with increasing anionic lipid content of the vesicles. For both peptides this increase was maximal at 50–60% DOPG. Beyond this PG concentration, the fluorescence intensity decreased to lower values. This decrease is probably due
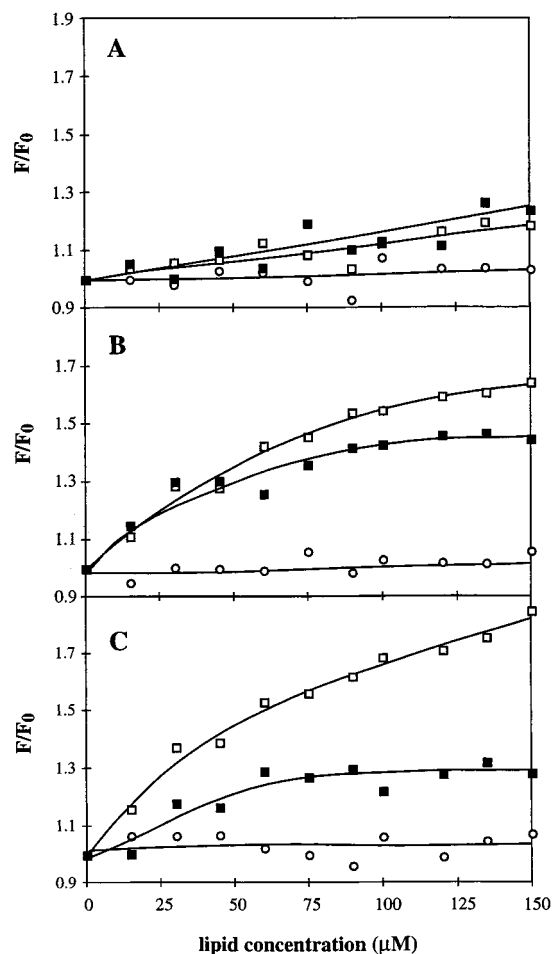


FIGURE 4: Fluorescence quantum yield of 1 $\mu$M nisin tryptophan mutant in the presence of vesicles of DOPC (○), DOPC/DOPG (1:1) (□), and DOPG (■) as a function of the lipid concentration. (A) 1W, (B) 17W, (C) 32W.

to quenching of the tryptophan fluorescence either by the phospholipid headgroup or due to self-quenching (see Discussion).

Titration of a solution of nisin tryptophan mutant with vesicles can give insight into the relative affinity of the peptide toward the different vesicle systems tested. The minor intensity changes of the three Trp-mutants in the presence of PC vesicles (Figure 4, open circles), of 1W in all systems and of 32W in the presence of pure PG vesicles, did not allow a reliable $K_d/n$ assessment. However, for 17W, $K_d/n$ values of 88 and 32 $\mu$M could be determined in the presence of PG/PC (1:1) and PG vesicles, respectively (Figure 4B, open and closed squares). 32W showed a similar affinity for the PG/PC (1:1) vesicles, i.e., 80 $\mu$M.

We did not observe a difference in interaction of the tryptophan variants with DOPC vesicles as compared to DOPC/DOPE (1:1) vesicles, upon titration of the vesicle to the peptides (not shown). The increased affinity of the tryptophan variants for vesicles containing increased amounts of anionic lipids, as was shown before for wild type nisin Z (9), provides further evidence that the tryptophan variants are valid representatives for wild type nisin Z.

*Acrylamide Quenching.* The blue-shifts of the tryptophan mutants indicated that they were inserted into the lipid phase of the membrane. This can be assessed in a more direct manner by means of acrylamide, a neutral water soluble
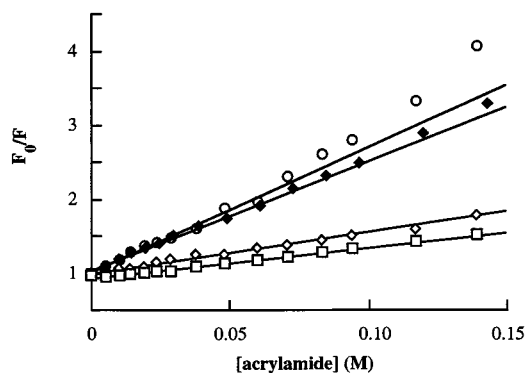
FIGURE 5: Stern−Volmer plot, showing the tryptophan fluorescence quenching by acrylamide of 1 $\mu$M 17W in buffer ($\blacklozenge$) and in the presence of 150 $\mu$M (lipid-Pi) vesicles of DOPC ($\bigcirc$), DOPC/DOPG (1:1) ($\Diamond$), and DOPG ($\square$).

Table 3: The Stern−Volmer Quenching Constants ($M^{-1}$) for 1.0 $\mu$M Nisin Mutant in the Absence or the Presence of Vesicles (150 $\mu$M Lipid-Pi) of Different Composition

|      | no lipid | DOPC | DOPC/DOPG (1:1) | DOPG |
|------|----------|------|-----------------|------|
| 1W   | 15.2     | 15.0 | 6.6             | 4.8  |
| 17W  | 14.9     | 16.4 | 5.6             | 3.7  |
| 32W  | 12.4     | 11.9 | 3.8             | 3.8  |

quencher of the tryptophan fluorescence. This quencher has the advantage that no charge interactions take place with the headgroups of negatively charged lipids, which may be the case for the often used iodide. We studied the acrylamide quenching in the presence of pure DOPC, DOPG/DOPC (1:1), and pure DOPG vesicles. Figure 5 shows the Stern−Volmer plot of the aqueous quenching by acrylamide of 17W. The tryptophan residue of 17W was readily quenched by acrylamide when the peptide was in buffer (closed diamonds) and in the presence of pure PC vesicles (open circles). Protection of quenching by acrylamide was observed in PG-containing vesicles. 1W and 32W showed similar quenching profiles for the three lipid systems tested (not shown). From these quenching profiles, the Stern−Volmer quenching constants ($K_{SV}$) were obtained as described in the Materials and Methods (Table 3). This Stern−Volmer constant is a measure for the accessibility of the tryptophan residue for the quencher. The $K_{SV}$ values for 1W, 17W, and 32W in the presence of PG-containing vesicles are significantly lower as compared to the $K_{SV}$ value in the presence of DOPC vesicles, indicating that the tryptophan residues are more protected against quenching by acrylamide. For 1W and 17W, the $K_{SV}$ values in the presence of pure DOPG vesicles are lower as compared to the $K_{SV}$ values in the presence of the mixed PG/PC system. These data clearly indicate that in the presence of negatively charged lipids the tryptophan residues at the three different sites of the nisin molecule are inserted in the bilayer.

*Quenching by Spin-Labeled Lipids.* To asses the depth of insertion, quenching experiments were performed with spin-labeled lipids. Spin-labels located at three different positions in the bilayer were used, i.e., one in the headgroup (0-SLPC), one at position 5, and one at position 12 of the acyl chain (5-SLPC and 12-SLPC, respectively). Upon insertion of a tryptophan residue in the lipid bilayer, the fluorescence intensity in the presence of vesicles containing spin-labels will become reduced as compared to the fluo-
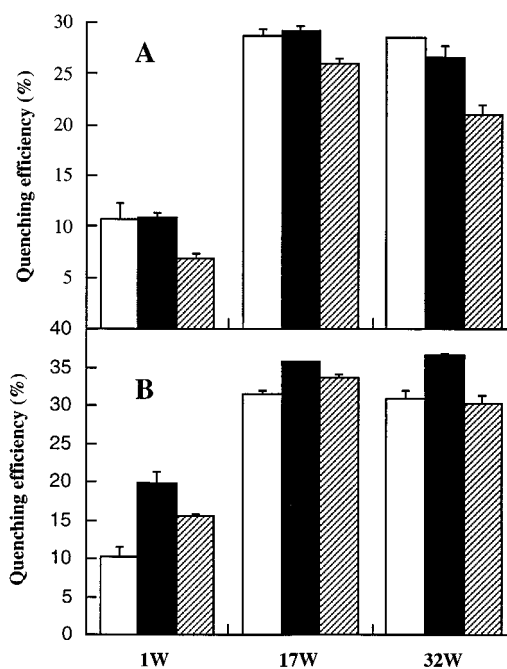


FIGURE 6: Quenching efficiency of the fluorescence of the nisin tryptophan mutants by spin-labeled lipids incorporated at 10 mol % in DOPG/DOPC (1:1) vesicles (A) and in DOPG/DOPC (9:1) vesicles (B). 0-SLPC open bars, 5-SLPC closed bars, 12-SLPC hatched bars, error bar: $n = 3$.

rescence in the presence of vesicles of the same composition, but without spin-labels. Figure 6 shows the results of such experiments for DOPG/DOPC (1:1) and DOPG/DOPC (9:1) vesicles, respectively, each containing 10 mol % spin-labeled PC.

For the equimolar vesicles, the tryptophan residues at the three different positions show comparable quenching profiles (Figure 6A). 1W shows the most quenching with the spin-labels 0-SLPC (open bars) and 5-SLPC (black bars), while with 12-SLPC (hatched bars), the least quenching is observed. A similar picture is observed for 17W. 32W slightly deviates from this picture. For the tryptophan residue at this position the most effective quencher is 0-SLPC, intermediate quenching is observed for 5-SLPC and the least quenching for 12-SLPC. These data suggest that the tryptophans at positions 1 and 17 are more deeply inserted into the membrane as compared to the tryptophan at position 32. For the PG/PC (9:1) vesicles, a different quenching profile is observed (Figure 6B). In this case, for all three tryptophan positions, the most efficient quencher is 5-SLPC (Figure 6B, black bars). For 17W and 32W the quenching efficiency of the 0-SLPC and the 12-SLPC are almost equal. For 1W the quenching profile is different, i.e., the 12-SLPC quenches more efficient as compared to the 0-SLPC. This suggests that the tryptophan of 1W is more deeply embedded in the lipid bilayer as compared to the tryptophan of 17W. Comparing the two lipid systems clearly shows that an increased amount of negatively charged lipids results in a deeper insertion of nisin in the membrane. Furthermore, the overall quenching efficiency in the presence of 90% DOPG was higher than in the presence of 50% DOPG. In both lipid systems the quenching efficiencies obtained with 1W are a factor of 2−3 smaller as compared to the other two peptides.

The presence of a membrane potential has been shown to promote the activity of nisin both in vivo and in vitro (*5, 7, 9, 31, 32*). We tested with use of the spin-labeled vesicles whether the presence of a membrane potential had an effect on the orientation of nisin. No effect of a membrane potential on the quenching of the tryptophan fluorescence could be observed for both lipid systems containing either one of the three spin-labeled PCs. This indicates that the membrane potential had no effect on the orientation of nisin. The possibility remains that initially the membrane potential induced a reorientation of nisin, but that this reorientation was transient, possibly due to the dissipation of the membrane potential by nisin induced pores, and occurred within the dead time of the experiments (6−10 s).

## DISCUSSION

To determine the orientation of nisin in the phospholipid bilayer, we prepared three tryptophan-containing nisin Z analogues with an unique tryptophan residue at positions 1, 17, or 32.

It was shown that the substitution of the different residues of nisin Z for a tryptophan did not largely affect the antimicrobial activity both in MIC assays and model systems. The largest difference in activity was found for the 32W-induced CF-leakage as compared to wild type nisin-Z-induced CF-leakage. Since 32W-induced $K^+$-leakage was similar to wild type-induced leakage, this may reflect a partial closure of the pore by the tryptophan at the C-terminus, thereby reducing the passage of larger molecules.

The blue-shifts of the emission maxima in the presence of negatively charged lipids containing vesicles suggest that the tryptophan residues of 1W, 17W, and 32W are at least partially inserted into the hydrophobic lipid phase of the bilayer. The larger blue shifts of the tryptophan residues in the presence of pure PG vesicles as compared to the mixed PG/PC (1:1) system suggest a deeper insertion with increasing PG concentration. These results fit well with the observed increase in monolayer insertion of nisin Z with increasing concentration of PG (*9*). Comparing the blue-shifts of the individual peptides suggests that the tryptophan at position 1 which has the largest blue-shift is probably more deeply inserted into the membrane than the tryptophans at positions 17 or 32.

It has been shown that sulfur atoms can quench the fluorescence of tryptophan residues when they are in close proximity (<7 Å) (*33, 34*). This effect can explain our observations for the 1W variant which displayed the lowest fluorescence intensity increase upon interaction with vesicles containing anionic lipids and, in the spin-labeled lipid experiments, displayed the lowest quenching efficiency. It has been shown that the largest changes in conformation upon interaction of nisin with SDS or DPC micelles take place at the N-terminus (*35*). From an analysis of the NMR structures of nisin in water and in the presence of DPC micelles, we have determined that such a conformational change would bring the tryptophan residue at position 1 substantially closer to the sulfur of the first lanthionine ring. This distance was estimated to be 12 Å in water and 7 Å in the prescence of DPC micelles, thus, close enough to cause quenching. Interestingly, we observed (not shown) that the I1W variant showed a lower quantum yield than the I1W/

Dhb2T analogue. This can be explained in the same context of a conformational change in the N-terminus due to the presence of the double bond at position 2 in I1W, but not in I1W/Dhb2T. This double bond causes a conformational constraint in the N-terminus of I1W, which is relieved in I1W/Dhb2T and moves the Trp side-chain away from the sulfur of the first lanthionine ring.

The fluorescence intensities of 17W and 32W initially increased with an increasing negatively charged lipid content of the membrane, as expected. However, the intensities decreased when the anionic lipid content of the membrane further increased from 50 to 100%. Such a behavior has been shown before for model peptides containing a tryptophan residue (*26*). It was suggested by these authors that this decrease in fluorescence may be due to the quenching properties of the negatively charged headgroups. This was supported by the observation that TMA-DPH in POPS shows a 20% lower fluorescence than in POPC (*36*). Another possibility is that nisin begins to aggregate at the membrane surface when the negatively charged lipid content of the membrane increases from 50 to 100%. In these aggregates, the tryptophan residues can be in close proximity, leading to fluorescence self-quenching. Fluorescence self-quenching as a result of aggregation in the membrane has been proposed before for the ionophore Lasalocid A (*37*) and the signal sequence of the *E. coli* precursor protein PhoE (*38*). There are indications that aggregation of nisin occurs at the membrane (*9, 39*); this makes the latter possibility more likely.

The $K_{SV}$ values of the fluorescence quenching by acrylamide in buffer are comparable with $K_{SV}$ values of acrylamide quenching obtained for other peptides. For mellitin, a $K_{SV}$ value in buffer was obtained of 12.5 $M^{-1}$ (*40*), while for small tryptophan-containing peptides, values of 12−17 $M^{-1}$ were obtained (*26*). This shows that the tryptophan residues are readily accessible in buffer, indicating that the nisin variants are not aggregated in buffer. No protection of the tryptophan fluorescence against quenching by acrylamide could be detected in the presence of PC vesicles. This is due to the lack of affinity of nisin for PC-vesicles as reported previously (*9*). The binding isotherms of 17W and 32W suggest that above a lipid concentration of 100 $\mu$M the binding of the peptides is saturated for the pure PG system, while in the presence of the mixed PG/PC (1:1) vesicles, the binding is not completely saturated. This would implicate that contibutions of unbound peptides are present in the fluorescence spectra of the tryptophan variants. However, binding experiments performed with wild type nisin Z under similar conditions showed that >80% of the peptides is bound in the mixed PG/PC (1:1) system while >90% is bound in the pure PG system (*9*). Therefore, the contributions of the unbound peptides in the spectra are relatively small, and we chose not to correct for this. Furthermore, the protection of the tryptophan residues in the presence of negatively charged lipids indicate that the tryptophan residues are inserted into the membrane in an anionic lipid-dependent way.

From of the quenching data from the spin-labeled lipid experiments, we calculated the depth of insertion for the three different tryptophan positions according to the two methods described in the Materials and Methods (Table 4). Both

Table 4: Most Probable Distances (Å) of the Tryptophan Residues to the Bilayer Center as Determined by the Parallax and the Distribution Analysis Method

|       | DOPG/DOPC (1:1) vesicles | | DOPG/DOPC (9:1) vesicles | |
|-------|----------------------|-----------------------|----------------|-----------------------|
|       | parallax[a]          | distribution analysis | parallax       | distribution analysis |
| 1W    | $15.8 \pm 0.3$       | $15.7 \pm 1.0$        | $9.9 \pm 0.4^b$ | $10.8 \pm 0.1$       |
| 17W   | $15.7 \pm 0.3$       | $15.0 \pm 0.6$        | $12.2 \pm 0.1^c$ | $11.5 \pm 0.2$      |
| 32W   | $16.2 \pm 0.2$       | $18.4 \pm 1.8$        | $12.6 \pm 0.3^c$ | $13.1 \pm 0.2$      |

[a] The distances were calculated using the spin-label pair 0-SLPC and 5-SLPC. [b] The distances were calculated using the spin-label pair 5-SLPC and 12-SLPC. These spin-label pairs were chosen since they were the two most efficient quenchers of the tryptophan fluorescence in the respective experiments. [c] The distances were calculated using the spin-label pairs 0–5 and 5–12, and the results of the two calculations were averaged (28).

methods show that in the presence of 90% DOPG nisin is more deeply inserted (~5 Å) in the membrane than in the presence of vesicles containing 50% DOPG. This deeper insertion of nisin with increasing negatively charged lipid content is possibly due to the stronger interactions of the positively charged lysine residues with the anionic phospholipid headgroups, which pull the peptide more deeply in the membrane. Such behavior was shown before for melittin (40). In the presence of 50% PG, both methods place the tryptophans of 1W and 32W at approximately the same depths. In the presence of 90% PG, the results of the calculation differ slightly between the two methods, although the observed trends remain the same, i.e., the tryptophan of

1W is calculated to possess the deepest location, while the C-terminal tryptophan of 32W has the shallowest location. In agreement with the observed largest blue-shift of 1W in pure PG vesicles, both methods of calculation place the N-terminus at the deepest location in the membrane, in the presence of 90% PG. In view of the slightly better correlation of the results from the distribution analysis with the quenching profiles, we used these results together with the family of NMR structures of nisin in the presence of DPC micelles (29) to estimate the actual orientation of nisin in the membrane (Figure 7). Only one structure complied with the criteria mentioned in the Materials and Methods. This structure was oriented so that the tryptophans at positions 1, 17, and 32 are positioned according to their depths relative to the bilayer center (straight line) for the 1:1 (panels A and C) and 9:1 (panels B and D) PG/PC system. As can be seen, nisin is, in both cases, oriented parallel to the bilayer surface, and the lysines are pointing outside the lipid–water interface (dashed line), which was set at 20 Å from the bilayer center. Figure 7 also gives a clear picture of the deeper insertion of nisin in the presence of 90% PG.

It may be argued that, due to the above-described quenching of the tryptophan fluorescence of 1W by the sulfur atom of the first lanthionine ring; interpretation of the spin-label data of this peptide was not allowed. However, despite this quenching, still significant different quenching efficiencies were obtained for the different spin-labeled lipids, thus allowing for the analysis of the data.
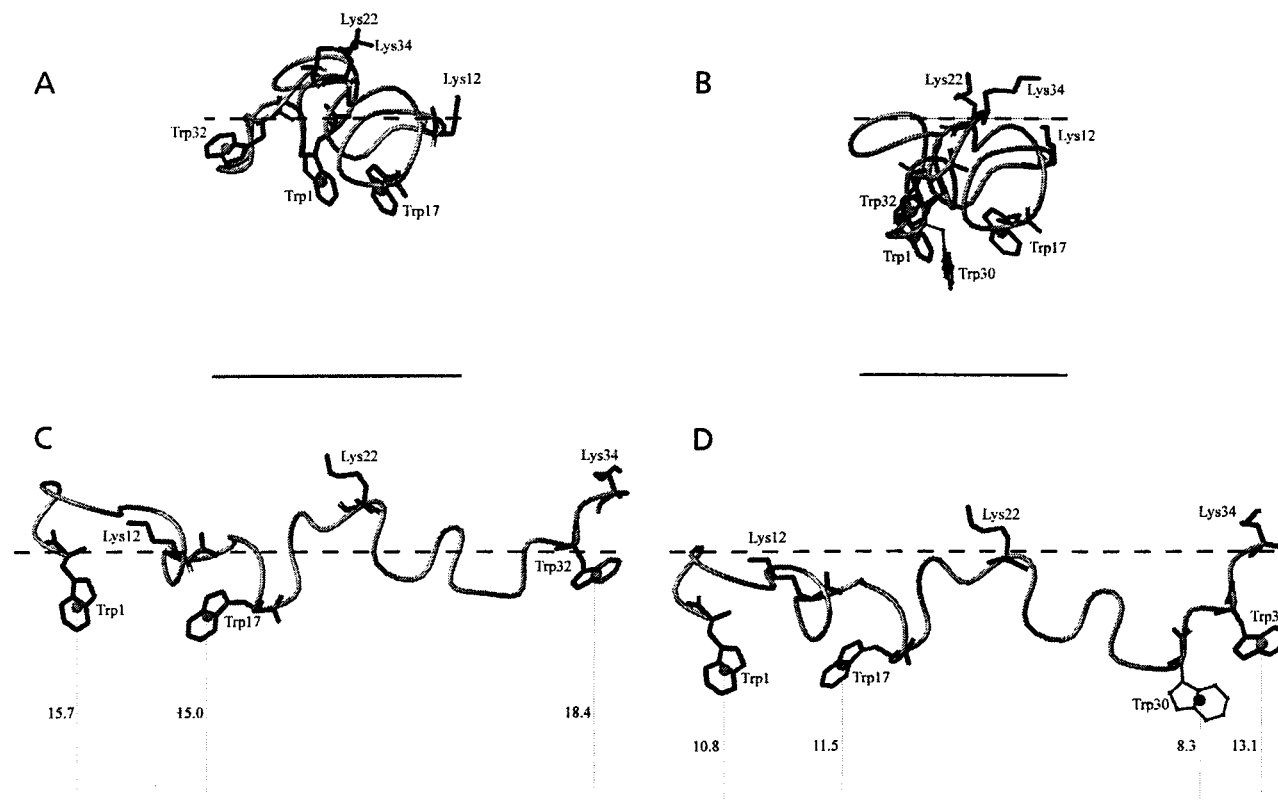


FIGURE 7: Modeling of the orientation of nisin in the membrane. Shown are backbone tracings of the nisin structure in the presence of 50% PG (A and C) and 90% PG (B and D), showing only the tryptophan and lysine residues. Panels A and B are views along the peptide axis, obtained by rotating panels C and D −90° in the y direction, with the C-terminus pointing outward. The larger dots in the tryptophan rings represent the centers of gravity of the tryptophan side chains which were used to position the tryptophans at their respective distance from the bilayer center (solid line). The dashed line represents the lipid water interface. See text for further details. The figure was drawn with the program MOLMOL (47).

Other information on the orientation of nisin at the lipid–water interface comes from NMR studies using spin-labeled fatty acids labeled at different depths in micelles of DPC. These studies indicated that nisin is immersed in the micel in an overall parallel orientation with respect to the micellar surface (*41*). Apparently, the orientation of nisin attached to micelles and the orientation of nisin in the membrane is quite similar.

Figure 7D furthermore shows that the extreme N-terminus of nisin is located in the membrane, while the extreme C-terminus is located in the water phase. This could explain earlier observations that showed that N-terminal extensions have large effects on the ability of nisin to insert into lipid monolayers (*12*). Moreover, a C-terminal extension of an aspartic acid residue and six histidines did not influence the ability of the peptide to insert into lipid monolayers (C. van Kraaij et al., unpublished observations). The location of the C-terminus in the water phase may explain the minor influence of a C-terminal extension on the monolayer insertion. Hence, the monolayer technique detects predominantly the insertion of the N-terminus as proposed earlier (*9*).

Recently, a fluorescence study with a nisin variant containing a tryptophan has been published (*11*). This study used nisin A, the other naturally occurring nisin variant (*42, 43*), with a tryptophan at position 30 (I30W). Interestingly similar to our results with 32W, for this peptide a reduced ability to induce leakage of calcein (a somewhat larger molecule than CF) was observed, while MIC-values did not show large differences. This may be caused by the above proposed partial closure of the nisin pore by the tryptophan at the C-terminus (now at position 30). These authors found a deeper location for the tryptophan at position 30 (3.6 Å from the bilayer center). This is significantly deeper as compared to our average depth of the three tryptophan residues of 11.8 Å. To test whether the cause of this difference is due to the relative position of the tryptophans in the molecule, we additionally placed a fourth tryptophan residue at position 30 in the above-described NMR structure. In Figure 7, panels B and D, it can be seen that Trp30 is indeed more deeply located than the other tryptophans, which clearly shows that the differences in depths of the tryptophan residues is mainly caused by their relative position in nisin. This demonstrates the importance of using multiple tryptophan mutants in these kinds of experiments, as well as the importance of modeling the results in combination with structural data, when available.

The overall parallel orientation of nisin seems to contrast pore formation of nisin in the membrane and would suggest that nisin causes membrane leakage by destabilizing the bilayer while remaining in a parallel orientation, as was proposed for other membrane-active peptides (*44*). However, recent experiments have shown that the C-terminal part of nisin translocates across the membrane, a process which is related to membrane permeabilization (C. van Kraaij et al., unpublished observations). This demonstrates that nisin must have obtained at some point in time a trans-bilayer orientation causing ion leakage (pore formation). However, the spin-label experiments show that these pores cannot be in a stable transmembrane orientation as has been proposed for alamethicin (*45*), but should be of transient nature. On the basis of the translocation experiments (C. van Kraaij et al., un-

published observations), the most likely event after transient pore formation by nisin is translocation of the whole molecule to the lumen of the vesicle as has been described for magainin (*46*). Thus, the stable parallel orientation accounts for nisin molecules at both sides of the vesicles. The role of the membrane potential remains unclear. The membrane potential may only accelerate the formation of pores (and in effect the translocation of the nisin molecules across the membrane) after which it is dissipated. This would not be detected by the fluorescence experiments with spin-labeled lipids. Furthermore, if aggregation of nisin indeed takes place in the presence of 90% PG, this would suggest that the nisin aggregates also have a stable parallel orientation with respect to the membrane surface. Aggregation of nisin in the membrane would be an important aspect in the mode of action and will be a topic for further investigation.

## REFERENCES

1. Delves-Broughton, J., Blackburn, P., Evans, R. J., and Hugenholtz, J. (1996) *Antonie van Leeuwenhoek 69,* 193−202.
2. Gross, E., and Morell, J. L. (1971) *J. Am. Chem. Soc. 93,* 4634−4635.
3. Jung, G. (1991) Lantibiotics: a survey in *Nisin and novel lantibiotics* (Jung, G., and Sahl, H.-G., Eds.) pp 1−31, ESCOM Science Publishers, Leiden.
4. Abee, T., Gao, F. H., and Konings, W. N. (1991) The mechanism of action of the lantibiotic nisin in artificial membranes in *Nisin and novel lantibiotics* (Jung, G., and Sahl, H.-G., Eds.) pp 373−385, ESCOM Science Publishers, Leiden.
5. Driessen, A. J. M., van den Hooven, H. W., Kuiper, W., Vandekamp, M., Sahl, H. G., Konings, R. N. H., and Konings, W. N. (1995) *Biochemistry 34,* 1606−1614.
6. Gao, F. H., Abee, T., and Konings, W. N. (1991) *Appl. Environ. Microbiol. 57,* 2164−2170.
7. Garcera, M. J., Elferink, M. G., Driessen, A. J., and Konings, W. N. (1993) *Eur. J. Biochem. 212,* 417−422.
8. Kordel, M., Schueller, F., and Sahl, H. G. (1989) *FEBS Lett. 244,* 99−102.
9. Breukink, E., van Kraaij, C., Demel, R. A., Siezen, R. J., Kuipers, O. P., and de Kruijff, B. (1997) *Biochemistry 36,* 6968−6976.
10. Giffard, C. J., Dodd, H. M., Horn, N., Ladha, S., Mackie, A. R., Parr, A., Gasson, M. J., and Sanders, D. (1997) *Biochemistry 36,* 3802−3810.
11. Martin, I., Ruysschaert, J. M., Sanders, D., and Giffard, C. J. (1996) *Eur. J. Biochem. 239,* 156−164.
12. Demel, R. A., Peelen, T., Siezen, R. J., de Kruijff, B., and Kuipers, O. P. (1996) *Eur. J. Biochem. 235,* 267−274.
13. Matsuzaki, K., Murase, O., Tokuda, H., Funakoshi, S., Fujii, N., and Miyajima, K. (1994) *Biochemistry 33,* 3342−3349.
14. Chung, L. A., Lear, J. D., and DeGrado, W. F. (1992) *Biochemistry 31,* 6608−6616.
15. Ren, J., Lew, S., Wang, Z., and London, E. (1997) *Biochemistry 36,* 10213−10220.
16. Liu, L.-P., and Deber, C. M. (1997) *Biochemistry 36,* 5476−5482.
17. Chattopadhyay, A., and London, E. (1987) *Biochemistry 26,* 39−45.
18. Kuipers, O. P., Rollema, H. S., Yap, W. M. G. J., Boot, H. J., Siezen, R. J., and de Vos, W. M. (1992) *J. Biol. Chem. 267,* 24340−24346.
19. Kuipers, O. P., Rollema, H. S., Beerthuyzen, M. M., Siezen, R. J., and de Vos, W. M. (1995) *Int. Dairy J. 5,* 785−795.

20. van Kraaij, C., Breukink, E., Rollema, H. S., Siezen, R. J., Demel, R. A., de Kruijff, B., and Kuipers, O. P. (1997) *Eur. J. Biochem. 247,* 114−120.

21. Ralston, E., Hjelmeland, L. M., Klausner, R. D., Weinstein, J. N., and Blumenthal, R. (1981) *Biochim. Biophys. Acta 649,* 133−137.

22. Hope, M., Bally, M. B., Webb, G., and Cullis, P. R. (1985) *Biochim. Biophys. Acta 812,* 55−65.

23. Rouser, G., Fleischer, S., and Yamamoto, A. (1970) *Lipids 5,* 494−496.

24. Lee, A. G. (1982) *Techniques in lipid and membrane biochemistry II,* Elsevier, Ireland.

25. Surewicz, W. K., and Epand, R. (1984) *Biochemistry 23,* 6072−6077.

26. de Kroon, A. I. P. M., Soekarjo, M. W., de Gier, J., and de Kruijff, B. (1990) *Biochemistry 29,* 8229−8240.

27. Eftink, M. R., and Ghiron, C. A. (1976) *J. Phys. Chem. 80,* 486-493.

28. Abrams, F. S., and London, E. (1993) *Biochemistry 32,* 10826−10831.

29. van den Hooven, H. W., Doeland, C. C. M., van de Kamp, M., Konings, R. N. H., Hilbers, C. W., and van de Ven, F. J. M. (1996) *Eur. J. Biochem. 235,* 382−393.

30. Jones, T. A., Zou, J.-Y., Cowan, S. S., and Kjeldgaard, M. A. (1991) *Acta Crystallogr. Sect. A 47,* 110−119.

31. Ruhr, E., and Sahl, H. G. (1985) *Antimicrob. Agents Chemother. 27,* 841−845.

32. Sahl, H. G., Kordel, M., and Benz, R. (1987) *Arch. Microbiol. 149,* 120−124.

33. Cowgill, R. W. (1967) *Biochim. Biophys. Acta 140,* 37−44.

34. Cowgill, R. W. (1970) *Biochim. Biophys. Acta 207,* 556−559.

35. van den Hooven, H. W., Fogolari, F., Rollema, H. S., Konings, R. N. H., Hilbers, C. W., and van de Ven, F. J. M. (1993) *FEBS Lett. 319,* 189−194.

36. Yeager, M. D., and Feigenson, G. W. (1990) *Biochemistry 29,* 4380−4392.

37. Chattopadhyay, A., Komath, S. S., and Raman, B. (1992) *Biochim. Biophys. Acta 1104,* 147−150.

38. Killian, J. A., Keller, R. C. A., Struyvé, M., de Kroon, A. I. P. M., Tommassen, J., and de Kruijff, B. (1990) *Biochemistry 29,* 8131−8137.

39. Giffard, C. J., Ladha, S., Mackie, A. R., Clark, D. C., and Sanders, D. (1996) *J. Membrane Biol. 151,* 293−300.

40. Batenburg, A. M., Hibbeln, J. C. L., Verkleij, A. J., and de Kruijff, B. (1987) *Biochim. Biophys. Acta 903,* 155−165.

41. van den Hooven, H. W., Spronk, C. A. E. M., Vandekamp, M., Konings, R. N. H., Hilbers, C. W., and van de Ven, F. J. M. (1996) *Eur. J. Biochem. 235,* 394−403.

42. Buchman, G. W., Banerjee, S., and Hansen, J. N. (1988) *J. Biol. Chem. 263,* 16260−16266.

43. Mulders, J. W., Boerrigter, I. J., Rollema, H. S., Siezen, R. J., and de, V. W. (1991) *Eur. J. Biochem. 201,* 581−584.

44. Bechinger, B. (1997) *J. Membr. Biol. 156,* 197−211.

45. He, K., Ludtke, S. J., Huang, H. W., and Worcester, D. L. (1995) *Biochemistry 34,* 15614−15618.

46. Matsuzaki, K., Murase, O., Fujii, N., and Miyajima, K. (1995) *Biochemistry 34,* 6521−6526.

47. Koradi, R., Billeter, M., and Wüthrich, K. (1996) *J. Mol. Graphics 14,* 51−55.